Journal of The Electrochemical Society, **157** (7) K145-K151 (2010)
0013-4651/2010/157(7)/K145/7/$28.00 © The Electrochemical Society

Magnetic Study of Fe_3O_4 Nanoparticles Incorporated within Mesoporous Silicon

P. Granitzer,[a,*,z] K. Rumpf,[a,*] M. Venkatesan,[b] A. G. Roca,[c] L. Cabrera,[c] M. P. Morales,[c] P. Poelt,[d] and M. Albu[d]

[a]*Institute of Physics, Karl Franzens University Graz, A-8010 Graz, Austria*
[b]*Institute of Physics, Trinity College Dublin, College Green, Dublin 2, Ireland*
[c]*Instituto de Ciencia de Materiales de Madrid, Consejo Superior de Investigaciones Cientificas, Cantoblanco, 28049 Madrid, Spain*
[d]*Institute for Electron Microscopy, University of Technology Graz, A8010 Graz, Austria*

Porous silicon (PS) matrices with oriented, separated pores grown perpendicular to the surface are used as a template for the incorporation of magnetite nanoparticles. The Fe_3O_4 particles used for infiltration into the PS template are coated with oleic acid in a hexane solution and exhibit an average diameter of 8 ± 1.5 nm. The narrow size distribution and the superparamagnetic behavior at room temperature are interesting features of these nanoparticles. In addition, the use of PS as a template for the particle deposition influences and modifies the collective magnetic response of the nanoparticles. Especially, anisotropy between the two magnetization directions, magnetic field parallel and perpendicular to the surface, has been observed. Magnetite nanoparticles play a key role in medical applications, but also the magnetic properties of such a nanoparticle/PS system are of technical interest due to the transition between superparamagnetic and ferromagnetic behaviors. Temperature-dependent magnetization measurements are used to gain information about the magnetic interaction of the particles.
 [DOI: 10.1149/1.3425605]

Manuscript submitted September 21, 2009; revised manuscript received March 31, 2010. Published May 12, 2010.

The fabrication of low dimensional systems as ultrathin layers, nanowires, nanoparticles, and nanodots is a key trend in today's nanotechnology. Not only the change in the physical properties of low dimensional materials compared to their bulk materials is of interest; their applicability is also a developing subject. Magnetic materials in the nanoscale range are utilized in magnetic data storage, giant magnetoresistance devices; magnetic particles are also employed in biological and medical applications.

The fabrication of isolated magnetic nanoparticles is difficult to reach because the large surface areas compared to the volume oxidize easily when using metals and due to the tendency of nanoparticles to agglomerate. A controlled passivation of the particles can be carried out, but this can also lead to interactions between the metal core and the passivating materials. Magnetic iron oxide such as magnetite has the advantage of being more stable. Recently, a new preparation method has been reported based on the decomposition at high temperatures of an organic precursor in the presence of oleic acid, which leads to a monodisperse size distribution of nanoparticles isolated by an oleic acid layer of around 2 nm.[1-3]

The dispersion of magnetite in a liquid carrier used for versatile applications, especially in biomedicine, has recently been studied.[4-6] The surface of the particles has been modified by biocompatible substances, and the magnetic interactions have been investigated.[7] Furthermore, the magnetic properties of magnetite nanoparticles embedded in a nonmagnetic matrix have been figured out in special ferromagnetic (FM) resonance studies, which show the dependence of the magnetic behavior on the utilized matrix material.[8] Furthermore, magnetite nanoparticles are extensively used for potential biomedical applications such as imaging of diseases (e.g., cancer and diabetes) or cellular therapy.[9] Magnetite nanoparticles self-assembled on porous silicon (PS) in a dendritic arrangement have been investigated concerning the self-organization process as well as the magnetic properties.[10]

The combination of nanostructured silicon and magnetite not only leads to interesting magnetic properties of the nanocomposite system but is also a good candidate for applications in biomedicine because both are biocompatible in biological systems due to their low toxicity and biodegradability.[11,12]

In the present work, PS fabricated in a self-organizing electrochemical procedure with dimensions in the mesoporous regime is used as a matrix for the incorporation of very uniform Fe_3O_4 nanoparticles with an average size of 8 nm. A magnetic characterization of this composite material sheds light not only on the transition between FM and superparamagnetic (SPM) behaviors but also on the magnetic interaction between the particles. Furthermore, the influence of the silicon matrix on the magnetic behavior is figured out.

Experimental

A PS matrix, which acts as a template for the infiltration of magnetite nanoparticles, was fabricated by anodization of a highly doped n-type silicon wafer in a hydrofluoric acid solution (10 wt %).[13] When applying a constant current density of 120 mA/cm^2 for 10 min, a porous structure with oriented pores grown perpendicular to the wafer surface was achieved. Silicon etching was performed at room temperature. The average pore diameter of these templates was typically 80 nm, and the mean distance between the pores was 40 nm (Fig. 1). Figure 2 shows an enhanced cross-sectional region of Fig. 1b exhibiting the pores with an average diameter of 80 nm and a mean distance between the pores of 40 nm. The dendritic growth cannot be completely suppressed in this morphology range. The thickness of the investigated PS layer was about 40 μm. In this diameter range, the growth of the main pores in the (100) direction was accompanied by the growth of additional side pores in the (111) direction, which was favored by the remaining free carriers between the pores. If the distance between the pores does not exceed twice the thickness of the space charge region to a great extent, the length of these dendrites can be minimized to a length in the range of the pore radius, thus ensuring a clear separation of the pores. This behavior is important for magnetic measurements to be sure of the separation of the pores.

Magnetite nanoparticles of an average size of 8 nm were prepared by high temperature decomposition of organic iron compound precursors following previously reported works.[2] Magnetite nanoparticles were synthesized using iron acetylacetonate as a precursor and phenyl ether as a solvent. A mixture of 0.71 g of $Fe(acac)_3$ (2 mmol), 2.38 g of 1,2-hexadecanediol (10 mmol), 1.69 g of oleic acid (6 mmol), 1.60 g of oleylamine (6 mmol), and 20 mL of trioctylamine was added to a three-neck flask. Then, the mixture was heated under mechanical stirring and a flow of nitrogen gas until a temperature of 200°C was reached. This temperature was kept con-

* Electrochemical Society Active Member.
[z] E-mail: petra.granitzer@uni-graz.at

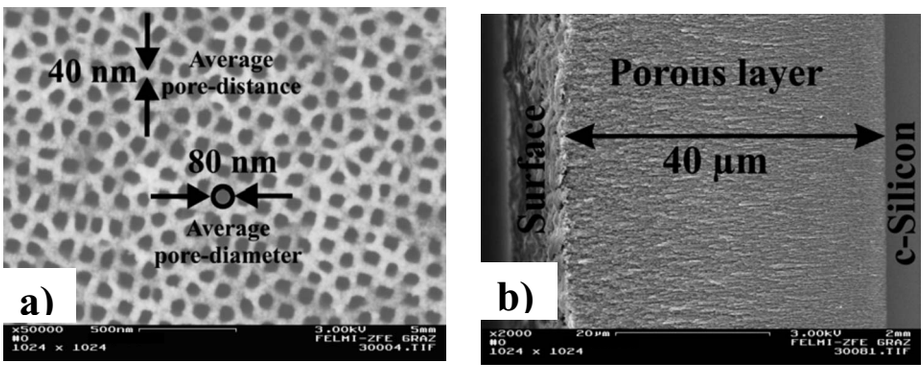

Figure 1. (a) SEM image of the top view of a PS matrix exhibiting an average pore diameter of 80 nm and a mean distance between the pores of 40 nm. (b) Cross-sectional micrograph showing the porous layer of about 40 µm with separated oriented pores grown perpendicular to the surface.

stant for 120 min, and then the solution was heated to reflux (369°C) for 30 min in a nitrogen atmosphere. Finally, the solution was cooled down to room temperature.

The powder was obtained by precipitation with ethanol, collected with a magnet, and finally dried under nitrogen flow. A stable suspension of the powder could be obtained when nanoparticles were mixed with 20 mL of hexane and 0.05 mL of oleic acid and were sonicated for a time period of 5 min. The achieved particles show a quite monodisperse size distribution (Fig. 3b) of 8 nm obtained from transmission electron microscopy (TEM) images (Fig. 3a) with a deviation of ±1.5 nm. The size distribution of the particles was obtained from images taking the distribution of the Fe content into account to improve the contrast of the TEM images.

The phase of iron oxide particles was identified by powder X-ray diffraction and IR spectroscopy. The X-ray patterns were collected in a Philips 1710 diffractometer using Cu Kα radiation. Fourier transform infrared (FTIR) spectra were recorded in a Nicolet 20 SXC FTIR. Samples were prepared by diluting the iron oxide powder in KBr at 2 wt % and following a compression of the mixture, pressing it into a pellet.

The suspension of magnetite nanoparticles in a hexane solution was infiltrated into the mesoporous silicon matrix (Fig. 4). This immersion was carried out under defined conditions, keeping the temperature constant at 25°C for an average time of 30 min. FTIR spectroscopy was performed to figure out the additional contribution of oleic acid and Fe–O to the absorption bands of PS.

Magnetization measurements of magnetite nanoparticles in powder form and after infiltration within PS were performed by superconducting quantum interference device magnetometry. The magnetic field was applied between ±1 T in two directions of magnetization, perpendicular and parallel to the sample surface, respectively, and the temperature was varied from 4.2 K up to room temperature. Zero field cooled (ZFC)/field cooled (FC) curves were registered at applied fields of 5500 and 1000 Oe.

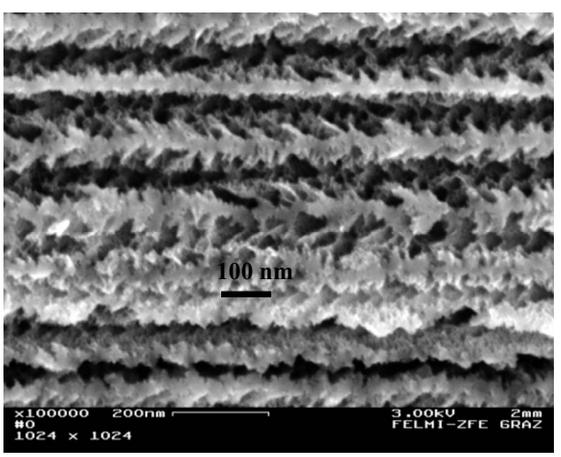

Figure 2. Cross-sectional micrograph showing an enhanced region of Fig. 1b. The oriented pores exhibit an average diameter of 80 nm, and the dendritic grown side pores do not exceed the length of distance between the pores, resulting in clearly separated pores.

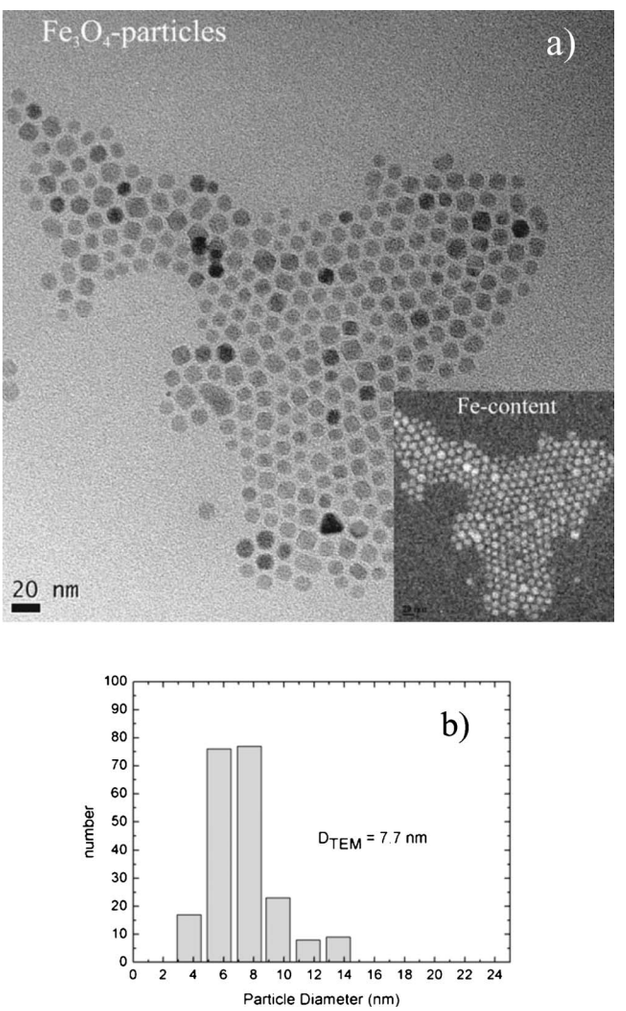

Figure 3. (a) TEM image of magnetite nanoparticles used for the infiltration into a PS matrix, which is shown in Fig. 1. (b) Histogram of the investigated Fe_3O_4 particles showing an average diameter of 7.7 nm with a deviation of ±1.5 nm and a low polydispersity index of 0.13. The size distribution is obtained from the element distribution of the Fe content [inset in (a)].

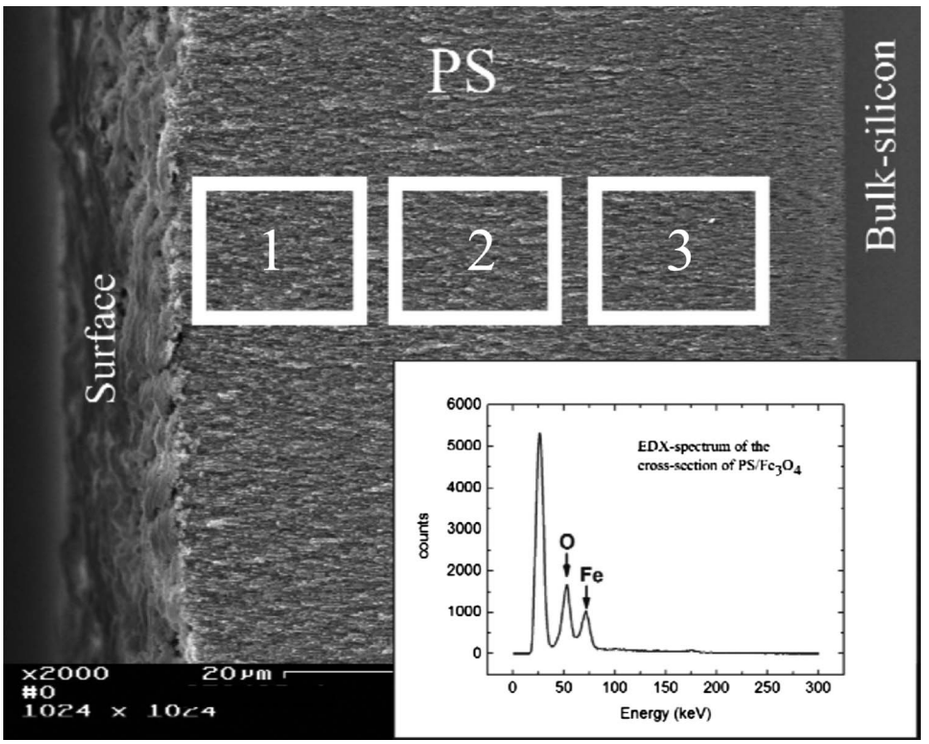

Figure 4. Cross-sectional view of a magnetite-filled PS specimen. The marked areas have been investigated by energy dispersive X-ray analysis spectroscopy. The iron and oxygen contents are, in all three regions, nearly the same. The spectrum of region 3 is shown in the inset.

Results and Discussion

The Fe_3O_4 particles coated with oleic acid in a hexane solution used for infiltration into the PS template exhibit an average diameter of 8 nm and only a distance of a few nanometers (~ 3 nm) between them (Fig. 3). Special features of these nanoparticles are the narrow size distribution as well as their SPM behavior at room temperature. X-ray diffractograms for Fe_3O_4 particles correspond to an inverse spinel structure with lattice parameters of 8.38(2) Å, which agrees with the published magnetite pattern (JCPDS 19-629) (Fig. 5). The IR spectrum for this sample presents two main absorption bands at around 600 and 400 cm^{-1} assigned to the Fe–O stretching modes of the magnetite lattice (Fig. 6).[14] In the high frequency range, bands associated with oleic acid molecules appear.

A comparison of a PS template and a PS/Fe_3O_4 sample has been figured out by FTIR spectroscopy (Fig. 7). In addition to the Si–H stretching modes of the PS, occurring in both samples, C–O stretching modes have been identified at 1530 and 1625 cm^{-1}, which agree with IR investigations of magnetite nanoparticles coated with oleic acid.[15] The shift of the peak position of bare oleic acid from 1715 cm^{-1} to lower wavenumbers is caused by the covalent bonding of the oleic acid molecules to the nanoparticle surface.[16] The Fe–O modes at 430 and 610 cm^{-1}, which has been observed in the absorption spectrum of the bare magnetite nanoparticles could not be found because of the absorption edge of the highly doped silicon substrate at 1200 cm^{-1}. Additional peaks at around 2260 cm^{-1} indicate an oxidation of the PS matrix [H–Si(O_3) modes].

The achieved magnetic system with PS acting as a substrate and infiltrated magnetite nanoparticles leading to a composite material shows an FM behavior at low temperatures ($T < T_B$) and superparamagnetism at higher temperatures ($T > T_B$). This transition temperature can be influenced not only by the particle size[16] but also

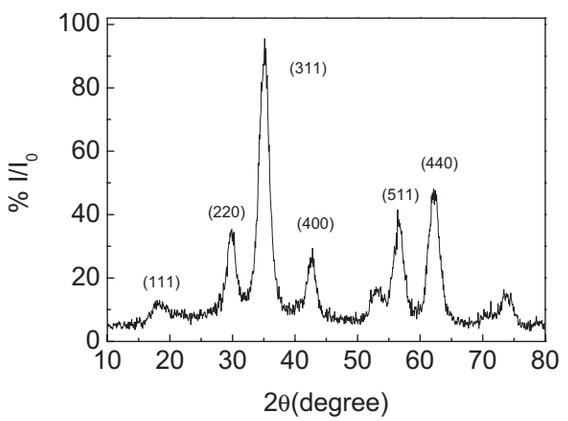

Figure 5. X-ray diffraction pattern for 8 nm iron oxide nanoparticles.

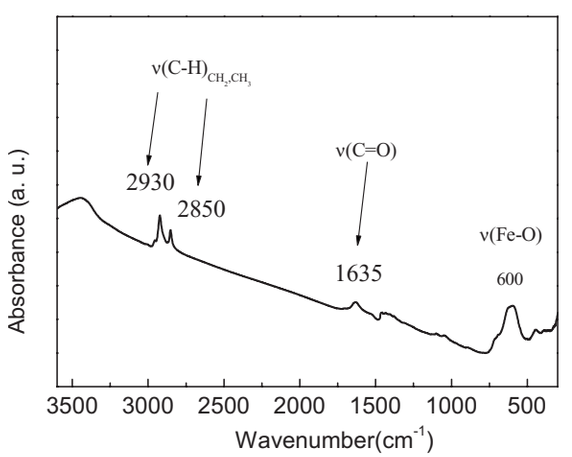

Figure 6. FTIR spectrum of Fe_3O_4 nanoparticles between 500 and 3500 cm^{-1} showing absorption peaks at around 600 cm^{-1}, which are assigned to the Fe–O stretching modes.

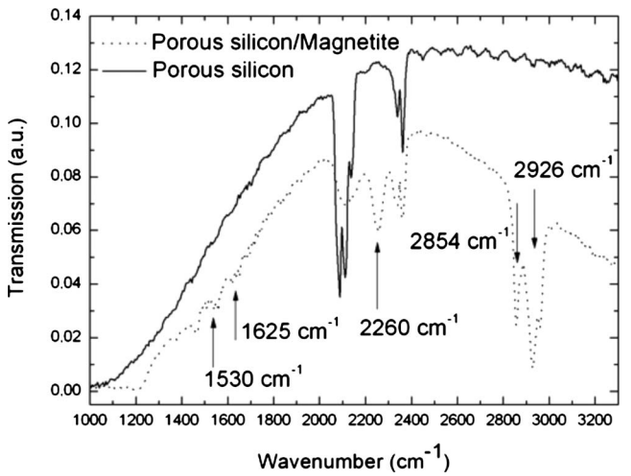

Figure 7. FTIR spectroscopy performed on a bare PS sample in comparison with a PS/magnetite specimen exhibiting an additional absorption band at 1530 cm^{-1} due to C–O stretching modes. At wavenumbers of 2854 cm^{-1}, CH_2 modes appear, and at 2926 cm^{-1}, modifications of SiO_x modes are observed. The Si–H stretching modes at around 2100 cm^{-1} decrease, and additional peaks at around 2260 cm^{-1} occur, which are due to the oxidation of the PS matrix [H–Si(O_3) modes].

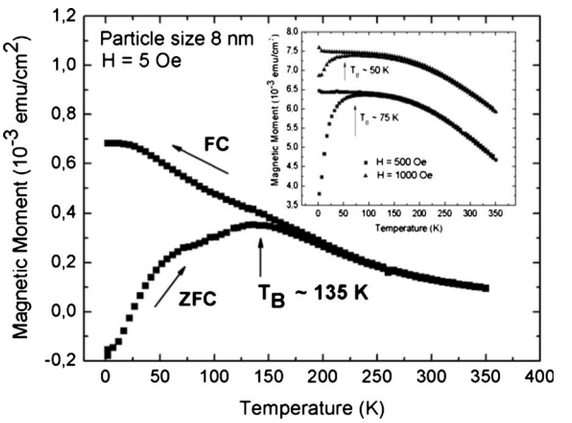

Figure 9. ZFC/FC measurements of Fe_3O_4 particles infiltrated into PS carried out at an applied magnetic field of 5 Oe and in a temperature range between 4.2 and 360 K. The blocking temperature (maximum peak of the ZFC branch) at 135 K indicates dipolar coupling between the particles. Inset: Shift of T_B toward lower temperatures with increasing applied magnetic field from about 135 K (H = 5 Oe) to 75 K (H = 500 Oe) and 50 K (H = 1000 Oe).

by the distance between the particles or by the concentration of the particle solution (Fig. 8). This distance can be varied by the coating used, which influences the magnetic particle–particle interaction within the individual pores. Furthermore, the interaction between adjacent pores can be modified by the thickness of the remaining silicon matrix. The following investigations have been performed by using a matrix with a typical mean distance of 40 nm between the pores.

The SPM behavior of the magnetite/PS system above a blocking temperature T_B is shown by temperature-dependent magnetization measurements. ZFC/FC investigations performed at an applied field of 5 Oe show a rather high blocking temperature T_B at 135 K, which indicates magnetic interactions between the particles (Fig. 9). Similar findings of T_B are reported in Ref. 17. Furthermore, a shift in the blocking temperature to lower temperatures with higher applied fields is observed (inset in Fig. 9). This behavior of SPM particles is proportional to $H^{2/3}$ (H magnetic field) at high fields and proportional to H^2 for lower fields.[18]

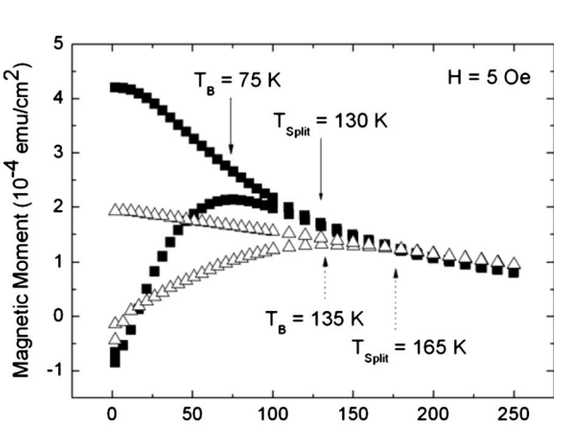

Figure 8. Temperature-dependent magnetization measurements of PS samples infiltrated with a Fe_3O_4 solution of different concentrations. Triangles: Specimen filled with a solution of initial concentration. Squares: Specimen filled with a magnetite solution of less (50%) concentration. The particle size is always the same.

Considering the ZFC/FC measurements, one recognizes that the splitting temperature between the ZFC and FC branches differs from the blocking temperature, which coincides with the maximum of the ZFC curve. Such a behavior is observed in randomly dipolar coupled nanomagnet systems.[19] Also, the width of the peak of the ZFC branch can be attributed to the dipolar coupling of the nanoparticles because the distribution of the particle size is quite monodisperse proofed by TEM images (Fig. 3).

The transition between SPM and stable behaviors occurs when the thermal energy barrier KV becomes equal to 25 k_BT,[20] where K is the anisotropy energy per unit volume of the SPM particle and V is its volume. For particles exhibiting a monodisperse size distribution, the blocking temperature T_B gives the threshold between stable ($T < T_B$) and unstable ($T > T_B$) regions.

The particle size is known from TEM images (average 8 nm), and thus the blocking temperature T_B can be estimated by the equation $KV = 25k_BT_B$. By taking $K = 1.35 \times 10^4$ J m^{-3} for Fe_3O_4,[21] this equation yields a value of $T_B = 10$ K by assuming a spherical shape of the particles on the basis of Fig. 3a. This T_B value is far away from the measured blocking temperature of 135 K by ZFC/FC measurements (Fig. 9). An implication is the loss of validity of the used equation for noninteracting particles; thus, a magnetic interaction (dipolar) between the iron oxide particles can be concluded. Consequently, it can be said that the particles of the investigated samples are SPM only above a quite high blocking temperature of 135 K due to the presence of dipolar interactions. Kechrakos and Trohidou,[22,23] Allia et al.,[24] and Gross et al.[25] showed that the blocking temperature is always enhanced due to interactions between the magnetic particles because the coupling suppresses the thermal fluctuations of the spins. Also, a broadening of the ZFC peak is observed due to magnetic interactions.[25] The higher measured blocking temperature of about 135 K than the one estimated from the equation above ($T_B = 10$ K) is no more valid for the ensemble of magnetically interacting particles investigated.

Considering the magnetization curve of magnetite nanoparticles (size 8 nm) without the PS matrix, one sees that the blocking temperature is 160 K and the bifurcation of the ZFC and FC branches takes place at 230 K (Fig. 10).

These temperatures are higher than in magnetite nanoparticles embedded in PS. Given that in both cases the same particles are

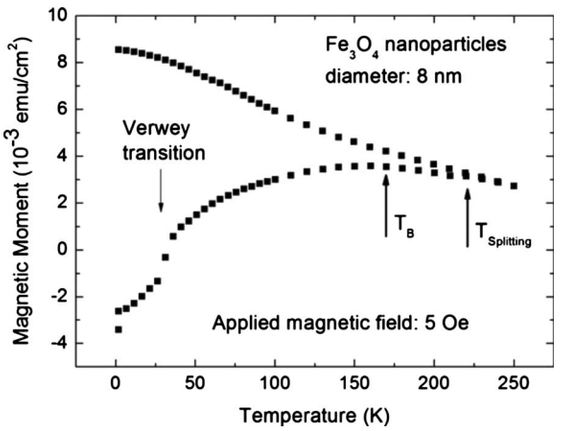

Figure 10. Temperature-dependent magnetization measurements of Fe_3O_4 nanoparticles exhibiting a blocking temperature at 160 K and a bifurcation of the two branches (ZFC/FC) at 230 K. The kink around 50 K is due to the Verwey transition of the magnetite nanoparticles.

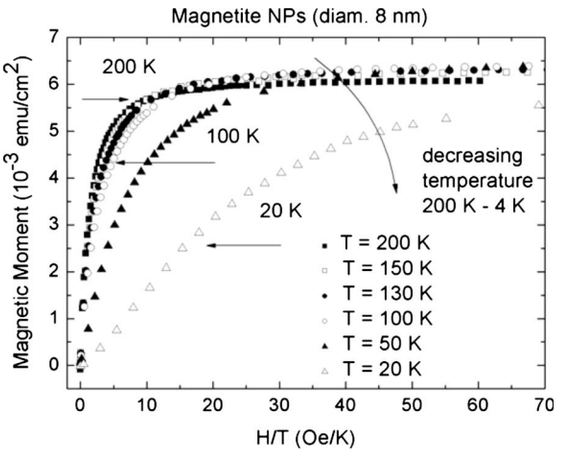

Figure 12. Magnetization curves of 8 nm bare magnetite nanoparticles vs H/T measured at various temperatures. The magnetization curves measured at 200, 150, and 130 K superimpose, whereas the measurements performed at lower temperatures deviate from the SPM behavior.

used, a reduction in the magnetic interaction can be assumed to take place when the magnetite nanoparticles are incorporated within the PS matrix, which is plausible to be caused by the morphology of the PS, exhibiting a distance between the pores (thickness of the remaining silicon pore walls) of about 40 nm. Thus, the interaction among the Fe_3O_4 nanoparticles in one direction along the pores is dominant. Moreover, due to the presence of oleic acid coating of the particles, the exchange interaction is discarded and the interaction is mainly dipolar. Figure 11 shows a scanning electron micrograph of the cross section of a magnetite-filled PS sample. The nanoparticles within the pores have an average diameter of 8 nm. The distance between the particles within one pore is given by the coating being a few nanometers, whereas the distance between adjacent pores is given by the morphology of the PS matrix, which is in this case about 40 nm (more than 10 times greater than the mean particle–particle distance given by the surfactant).

Further magnetization measurements have been performed to point out the transition between SPM and FM behaviors of the silicon/magnetite system in an H/T diagram. Considering the magnetization curves vs H/T of bare magnetite nanoparticles (8 nm), a superposition for temperatures from 200 down to 150 K has been observed (Fig. 12), which coincides with the ZFC/FC measurements. The PS/magnetite sample, infiltrated with the same nanoparticles, shows an SPM behavior up to 130 K (Fig. 13). This shift in the transition temperature between SPM and FM behaviors can be ascribed to the use of the PS matrix, which reduces the dipolar coupling due to the restriction of the nanoparticles within the oriented pores. A deviation from the superposition can arise from a broad particle-size distribution (which can be excluded in this case), anisotropy effects, or different spontaneous magnetizations of the particles with the temperature.[26]

An additional kink is observed in the ZFC curve for magnetite nanoparticles as synthesized and dispersed in the silicon matrix below 50 K, which could be assigned to the Verwey transition.[27] Considering 8 nm bare magnetite nanoparticles and the same particles infiltrated into a PS matrix, the Verwey temperature is shifted to higher temperatures (Fig. 14) from about 30 to about 50 K. The observed T_V between 30 and 50 K is high compared to the measurements done by Goya et al. on 47 nm magnetite nanoparticles exhibiting a T_V of around 16 K, whereas for smaller particle sizes this transition temperature could not be observed.[27] In that case, particles were prepared in water and were uncoated. Therefore, the aggregation state and the surface oxidation were completely different in those particles prepared in organic media in the presence of oleic acid.

The hysteresis loops of a bare silicon wafer the surface of which was covered with a suspension of Fe_3O_4 nanoparticles and a PS

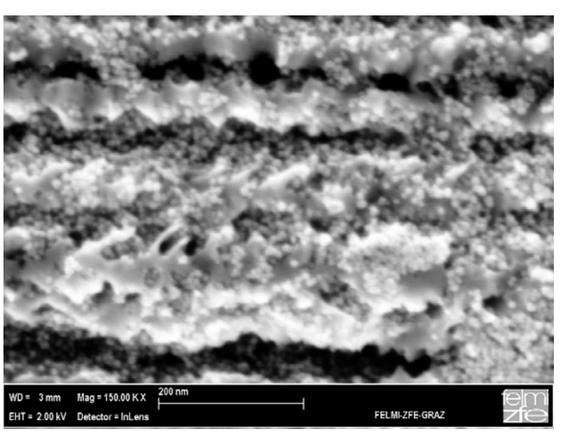

Figure 11. Scanning electron micrograph of a PS sample with infiltrated magnetite nanoparticles, showing the particles (about 8 nm) within the pores.

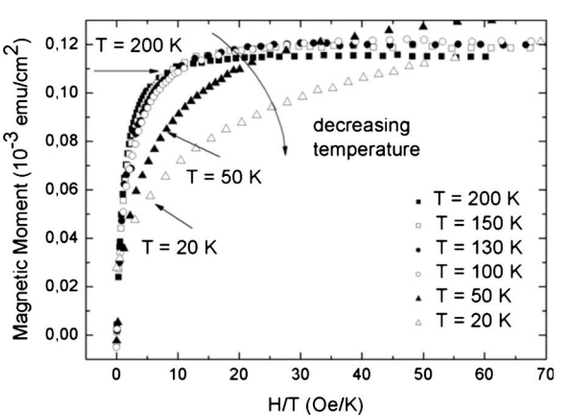

Figure 13. Magnetization curves of PS with infiltrated magnetite particles (8 nm). A superposition of curves measured between 200 and 100 K is observed.

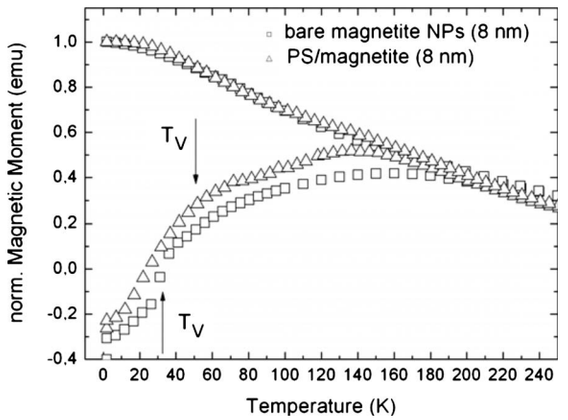

Figure 14. ZFC/FC measurements of bare magnetite nanoparticles and the same particles infiltrated into PS. The additional kink in the curve can be assigned to the Verwey temperature. A shift in T_V to higher temperatures is observed in the PS/magnetite composite.

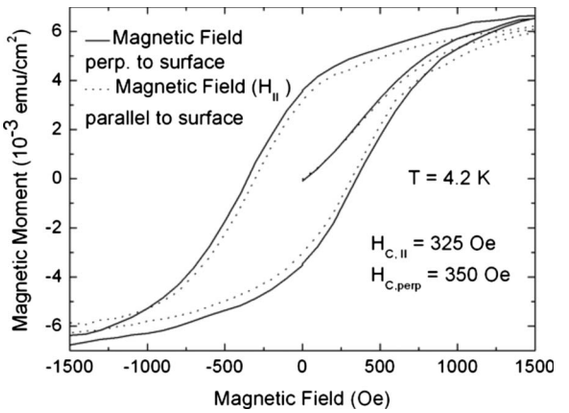

Figure 16. Hysteresis loops of a PS matrix impregnated with a magnetite solution. The measurements have been carried out for two directions of magnetization, perpendicular (full line) and parallel (dotted line) to the sample surface. The small anisotropy is caused by the morphology of the used PS template, leading to dominant coupling of particles situated along one pore. The coupling is of dipolar character.

matrix with magnetite nanoparticles impregnated into the PS layer are measured at $T = 4.2$ K. The magnetic field is applied perpendicular and parallel to the sample surface. The silicon wafer having the surface covered with the magnetite solution shows a magnetic anisotropy between the two magnetization directions (Fig. 15), which is similar to the behavior of a magnetic thin film due to the dipolar coupling of the nanoparticles.

Considering the hystereses loops of a PS specimen infiltrated with magnetite nanoparticles, the magnetic anisotropy between the two magnetization directions is weak (Fig. 16), but it differs drastically from the magnetization curve of a surface-covered bare silicon wafer (Fig. 15) using the same magnetite solution. The coercivities obtained for the two different magnetization directions vary a little ($H_{C\parallel} = 325$ Oe, $H_{C\perp} = 350$ Oe), which shows that the particles are mainly incorporated within the pores, and they do not accumulate on the surface of the PS template. The interaction between the particles occurs mainly within one pore (the minimum distance between the particles is twice the thickness of the coating) but less from one pore to another one (the average distance between the adjacent pores is about 40 nm). The PS specimens offering straight pores grown perpendicular to the surface are used as a matrix for the Fe_3O_4 nanoparticles and influence the magnetic behavior to a great extent. Also, the blocking temperature of the PS/magnetite nanocomposite is shifted to lower temperatures compared to the equal bare Fe_3O_4 particles.

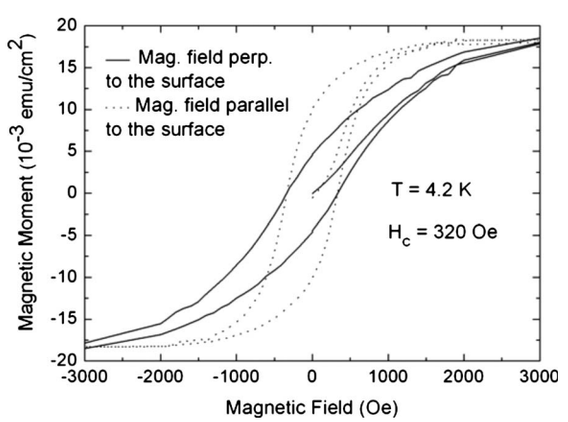

Figure 15. Magnetization measurements of a bare silicon wafer covered with magnetite nanoparticles are performed with the magnetic field applied perpendicular to the surface (full line) and parallel to the surface (dotted line), respectively. The obtained anisotropy is similar to that of a magnetic film, affirming that the Fe_3O_4 particles, which form a thin layer, exhibit a dipolar interaction.

Magnetite is nowadays investigated because of its promising applications in nanomedicine for the location and diagnosis of tumors. Due to the biodegradability and biocompatibility of PS,[12] a combination of these two materials is a promising candidate for medical in vivo applications. The magnetic properties of the nanoparticle/PS system are of interest due to the magnetic phase transition controlled by the strength of the magnetic interaction, which is determined by the distance between the particles and the direction, given by the matrix. Strongly interacting particles could lead to a blocking even at room temperature.

Conclusion

The infiltrated magnetite nanoparticles into the PS matrix are SPM at room temperature, and dipolar interactions are present. This behavior explains the high blocking temperature obtained from ZFC/FC measurements. Due to the infiltration of the particles into the oriented, separated pores of a PS layer, the interaction mainly takes place in one direction, reduced between the pores with respect to pure nanoparticles or a thin layer of particles formed on a wafer surface. An influence of the PS template can also be found in direction-dependent magnetization measurements resulting in a magnetic anisotropy. The obtained composite material consisting of a PS matrix and infiltrated Fe_3O_4 nanoparticles is an interesting system in nanotechnology applications due to the magnetic switching behavior and because of the transition between SPM and FM behaviors, which can be adjusted by modifying the distance between the particles. Moreover, the silicon substrate material is compatible with today's microtechnology. PS/magnetite systems are also interesting for medical applications because of the low toxicity of both materials.

Acknowledgments

This work is supported by the Austrian Science Fund (FWF) under project 21155. The work of Dr. Morales and Dr. Roca was supported by the Ministerio de Ciencia e Innovacion through the NAN2004-08805-C04-01 project. The authors thank Sanja Simic from the Institute of Electron Microscopy at the University of Technology Graz for her efforts in making scanning electron micrographs and Professor H. Krenn from the KF University Graz for making available experimental equipment.

References

1. T. Hyeon, S. S. Lee, J. Park, Y. Chang, and H. B. Na, *J. Am. Chem. Soc.*, **123**, 12798 (2001).
2. S. Sun and H. Zeng, *J. Am. Chem. Soc.*, **124**, 8204 (2002).
3. W. W. Yu, J. C. Falkner, C. T. Yavuz, and V. L. Colvin, *Chem. Commun. (Cambridge)*, **2004**, 2306.
4. O. Kuznetsov, N. Brusentsov, A. Kuznetsov, N. Yurchenko, N. Osipov, and F. Bayburtskiy, *J. Magn. Magn. Mater.*, **194**, 83 (1999).
5. *Scientific and Clinical Applications of Magnetic Carriers*, U. Haefeli, W. Schutt, J. Teler, and M. Zborowski, Editors, Plenum, New York (1997).
6. J. Lee, T. Isobe, and M. Senna, *J. Colloid Interface Sci.*, **177**, 490 (1996).
7. M. Mikhaylova, D. K. Kim, N. Bobrysheva, M. Osmolowsky, V. Semenov, T. Tsakalakos, and M. Muhammed, *Langmuir*, **20**, 2472 (2004).
8. N. Guskos, E. A. Anagnostakis, and A. Guskos, *J. Achievements Mater. Manufacturing Engineering*, **24**, 26 (2007).
9. J. R. McCarthy and R. Weissleder, *Adv. Drug Delivery Rev.*, **60**, 1241 (2008).
10. S. Balakrishnan, Y. K. Gun'ko, T. S. Perova, R. A. Moore, M. Venkatesan, A. P. Douvalis, and P. Bourke, *Small*, **2**, 864 (2006).
11. M. P. Pileni, N. Feltin, and N. Moumen, in *Scientific and Clinical Applications of Magnetic Carriers*, U. Häfeli, W. Schütt, J. Teller, and M. Zborowski, Editors, Plenum, London (1997).
12. L. T. Canham, in *Properties of Porous Silicon*, L. T. Canham, Editor, IEE, London (1997).
13. P. Granitzer, K. Rumpf, P. Poelt, A. Reichmann, and H. Krenn, *Physica E (Amsterdam)*, **38**, 205 (2007).
14. *The Iron Oxides: Structure, Properties, Reactivity, Occurrences and Uses*, R. M. Cornell and V. Schwertmann, Editors, VCH, Tokyo (1996).
15. A. G. Roca, M. P. Morales, K. O'Grady, and C. J. Serna, *Nanotechnology*, **17**, 2783 (2006).
16. J. Park, K. An, Y. Hwang, J. G. Park, H. J. Noh, J. Y. Kim, J. H. Park, N. M. Hwang, and T. Hyeon, *Nat. Mater.*, **3**, 891 (2004).
17. J.-H. Wu, S. P. Ko, H.-L. Liu, S. Kim, J.-S. Ju, and Y. K. Kim, *Mater. Lett.*, **61**, 3124 (2007).
18. G. F. Goya and M. P. Morales, *J. Metastable Nanocryst. Mater.*, **20–21**, 673 (2004).
19. J. D. Denardin, A. L. Brandl, M. Knobel, P. Panissod, A. B. Pakhomov, H. Liu, and X. X. Zhang, *Phys. Rev. B*, **65**, 064422 (2002).
20. B. D. Cullity and C. D. Graham, *Introduction to Magnetic Materials*, 2nd ed., John Wiley & Sons/IEEE, New York (2009).
21. J. Mazo-Zuluaga, J. Restrepo, and J. Mejía-López, *Physica B*, **398**, 187 (2007).
22. D. Kechrakos and K. N. Trohidou, *J. Magn. Magn. Mater.*, **262**, 107 (2003).
23. D. Kechrakos and K. N. Trohidou, *Phys. Rev. B*, **62**, 3941 (2000).
24. P. Allia, M. Coisson, M. Knobel, P. Tiberto, and F. Vinai, *Phys. Rev. B*, **60**, 12207 (1999).
25. A. F. Gross, M. R. Diehl, K. C. Beverly, E. K. Richman, and S. H. Tolbert, *J. Phys. Chem. B*, **107**, 5475 (2003).
26. D. L. Leslie-Pelecky and R. D. Rieke, *Chem. Mater.*, **8**, 1770 (1996).
27. G. F. Goya, T. S. Berquo, F. C. Fonseca, and M. P. Morales, *J. Appl. Phys.*, **94**, 3520 (2003).